Optical actuation of GeTe phase-change RF switches at 915nm: performance comparison for different GeTe sizes and impact of cycling

A. Naoui, I. Charlet, S. Guerber, B. Charbonnier, C. Dupré, J. Lugo, C. Héllion, M. Allain, B. Reig, Etienne Perret, et al.

Optical Actuation of GeTe Phase-Change RF Switches at 915nm: Performance Comparison for Different GeTe Sizes and Impact of Cycling

A. Naoui [#,$,*1], I. Charlet [#2], S. Guerber [#], B. Charbonnier [#], C. Dupré [#], J. Lugo [#], C. Héllion [#], M. Allain [#], B. Reig [#3], E. Perret [*], F. Podevin [$]

[#]CEA-LETI, Université Grenoble Alpes, F-38000 Grenoble, France
[$]Grenoble INP-UGA, TIMA, F-38031 Grenoble, France
[*]Univ. Grenoble Alpes, Grenoble INP, LCIS, F-26000 Valence, France
{[1]ayoub.naoui, [2]ismael.charlet, [3]bruno.reig}@cea.fr

***Abstract* — This paper presents GeTe-based switches for RF applications, reversibly switching between their ON and OFF states thanks to optical activation by irradiation. Contrarily to what has been presented so far, the transition is induced by infrared laser pulses, at λ = 915 nm which is very encouraging for future integration of laser sources and therefore for proposing a fully integrated optical actuation of PCMs switches. This is a new trend as compared to literature work dealing with the other side of the visible spectrum, less suited for optical integration on a die. Our work also reveals the effectiveness of wide and thick PCMs at this wavelength, enabling bi-stable switching at high frequencies up to 40 GHz, with a FoM of 31.5 fs attained despite a poor GeTe conductivity of only $1.85 \cdot 10^5$ S/m. Furthermore, significant progress as compared to the literature has been made by exceeding 30k cycles with optical actuation.**

***Keywords* — RF-switches, Phase change material (PCM), Germanium-Telluride (GeTe), Optical actuation, Infrared wavelength.**

I. Introduction

Phase Change Materials (PCMs) have a long history of application, traditionally used in memory [1] and the optical storage industry [2]. However, recent developments have brought PCM chalcogenides to the forefront as promising candidates for a new generation of radio-frequency (RF) switches. These PCM-based RF switches, such as germanium-telluride (GeTe) or germanium-antimony-telluride (GST), offer remarkable performance characteristics, including high power handling, low $R_{on}C_{off}$, the status of non-volatile switches, and reduced power consumption. They have become crucial in the context of modern RF applications [3], particularly in addressing issues related to millimeter-wave radars, 6G networks, and high-frequency communication [4][5][6].

Nevertheless, the activation of these PCM-based RF switches presents significant challenges. Conventional methods often rely on indirect heating, such as micro-heaters [7], which can induce parasitic capacitances limiting RF performance but also non-uniform temperature distribution alongside both the micro-heater and the PCM element [8]. This second point can also hurt RF performance, as any incomplete crystallization or amorphization of the PCM increases either the R_{on} or the C_{off}. Other solutions, such as optical actuation, have been considered [9][10][11], but have been hindered by the use of expensive UV lasers that are not compatible with CMOS photonics technology. In [11], optically controlled GeTe was used to reconfigure notch filters and polarizers in the THz frequency. A reconfigurable antenna is presented in [9], where GeTe deposits are used to connect or disconnect radiating elements. Finally, [10] presents a large-scale RF-PCM switch, whose performance has been characterized in frequency. None of these articles studies the impact of cycling, where only a very limited number of state changes have been implemented in practice without being able to give an idea of the evolution of performance as a function of the number of cycles. In this context, this work presents for the first time to our knowledge the optical actuation performance of GeTe RF switches of different sizes at an IR optical wavelength of 915 nm. The first part describes the optical actuation conditions of various GeTe sizes and their DC performance. The second part investigates their RF performance. The third part is dedicated to endurance tests. The last part is devoted to a comparison with state-of-the-art.

Table 1. Different devices of GeTe studied in this work.

Name	PCM length	PCM width	PCM thick	Optical fiber
DUT15_1	1 µm	5 µm	100 nm	Hi 780 ∅ 5 µm
DUT25_1	2 µm	5 µm	100 nm	Hi 780 ∅ 5 µm
DUT19_1	1 µm	9 µm	100 nm	SMF 28 ∅ 10 µm
DUT29_1	2 µm	9 µm	100 nm	SMF 28 ∅ 10 µm
DUT15_2	1 µm	5 µm	200 nm	Hi 780 ∅ 5 µm
DUT25_2	2 µm	5 µm	200 nm	Hi 780 ∅ 5 µm

Hi780 : high index fiber with operating λ of 780nm.
SMF28 : single mode fiber with operating λ between 1310 and 1550nm.

II. Optical Actuation of GeTe Material

A. Optical actuation

In this work, series RF switches integrated on a coplanar waveguide (CPW) are studied using GeTe with various widths,

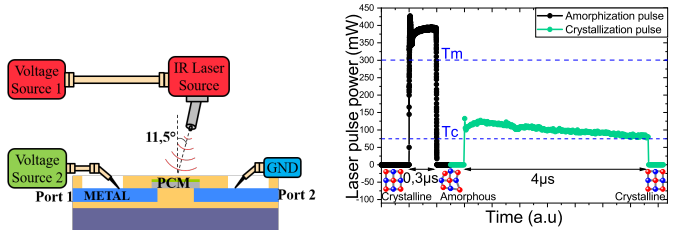

(a) (b)

Fig. 1. (a) Experimental setup for optical excitation; (b) Exemple of laser pulses used in this work for optical actuation

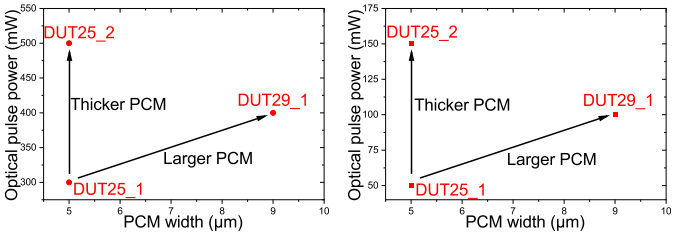

(a) (b)

Fig. 2. Required power for different PCM switches widths and thicknesses : (a) For amorphization; (b) For crystallization.

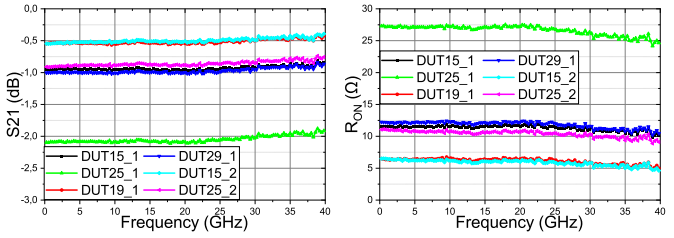

(a) (b)

Fig. 3. Crystalline GeTe RF performances for different sizes: (a) Insertion loss; (b) ON-state resistor.

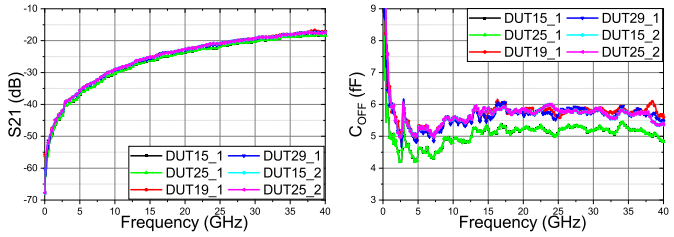

(a) (b)

Fig. 4. Amorphous GeTe RF performances for different sizes: (a) Isolation; (b) OFF-state capacitor.

lengths, and thicknesses (see Table 1 for a summary). Optical actuation is performed by direct irradiation through an optical fiber connected to a pulsed laser source operating at a wavelength of 915 nm, where the fiber is placed at a distance of 10 µm above the PCM element and with an angle of 11,5° to the surface normal, as shown in Fig. 1(a). Two types of optical fiber have been used with different diameters to address all the switch sizes (Table 1). Micropositioners on a standard Cascade automatic probe station enable the fiber to be aligned with PCM at the wafer level, offering light, scalable, and highly localized energy delivery to the PCM switches. These light pulses are absorbed by the material, causing localized heating within the PCM itself. The increase in temperature and the following cooldown induce a phase transition in the PCM, modifying its electrical properties, especially its resistance.

The devices are actuated with two types of optical pulses, as shown in Fig. 1(b). A short pulse (300 ns) is used to heat the GeTe above its melting temperature (Tm∼973 K). Immediately afterward, a thermal quench freezes the atoms in the amorphous state (OFF-state). Crystallization is achieved by applying a pulse of about 4 µs duration that heats the PCM above its recrystallization temperature (Tc∼573 K), at which crystal grain growth and nucleation are activated, changing the resistivity of the PCM from amorphous (high resistivity) to crystalline (low resistivity). To extract the PCM DC resistance at each state, a 2-probe measurement is performed by applying a 10 mV pulse with a Keithley B2902A source after each optical activation.

B. DC performance as a function of geometry

Fig. 2(a) shows the minimum power required to amorphize DUT25_1, DUT29_1, and DUT25_2, where increasing optical pulses with steps of 50 mW were applied until switching could be reached. When lengths and thicknesses are kept equal, it seems intuitive that a switch twice as wide requires twice as much power. This is not exactly the case in Fig. 2(a)when considering a ratio of surface between PCM and fiber of 51% for DUT25_1, leading to 153 mW of received power if the device were evenly illuminated and of 23% for DUT29_1, leading to 92 mW of received power if the device were evenly illuminated. The reason is the following: the smallest width is illuminated with a 5-µm fiber with a profile almost Gaussian, which means that light is localized in the middle. To guarantee a sufficient temperature at the edges of the sample, a higher laser power is therefore required. This is not necessary with a fiber of 10µm whose profile is almost multimode at 915 nm. Concerning thickness, theoretically, the required powers to switch are proportional to the GeTe volume. In particular, DUT29_1 and DUT25_2 have the same volume of GeTe, but higher powers are required to switch DUT25_2 (Fig. 2(a)). This can be explained by the fact that optical absorption follows an exponential decay with thickness. Fig. 2(b) leads to similar conclusions for crystallization.

III. Radio-Frequency Performances of PCM Switches

To evaluate the RF performance of optical switching, S-parameter measurements were carried out on all devices using a 2-port Keysight PNAX vector network analyzer. Calibration was carried out in the frequency range of 40 MHz - 40 GHz. Initially, the analysis focuses on switches in their ON-state (PCM optically crystallized). Fig. 3(a) illustrates the insertion losses measured after deembedding in this state for switches of different widths and thicknesses. The observations reveal that insertion losses are halved by doubling the PCM cross-section. These results are then used to extract

Table 2. Performances comparaison with the state-of-art.

Ref	Actuation	PCM size	PCM thick	R_{ON}_meas (Ω)	R_{ON}_cal (Ω)	C_{OFF} (fF)	FoM meas (fs)	Cycling
[9]	Optical	2x5 μm^2	100 nm	23	-	13.79	-	10
[10]	Optical 248nm	3x50 μm^2	200 nm	3	-	8.8	26	-
[11]	Optical 248nm	1.5x0.5 mm^2	500 nm	-	-	-	-	10
[5]	Electrical	0.9x30 μm^2	- nm	0.9	-	14.1	12.7	-
[12]	Electrical	2x10 μm^2	75 nm	4.5	-	35	149	-
[13]	Electrical	5x44 μm^2	150 nm	11.5	-	3.3	37	300k
[14]	Electrical	0.6x12 μm^2	250 nm	3.9	-	10.2	39.8	-
[15]	Electrical	3x- μm^2	- nm	4.5	-	5.6	25.2	10M
[16]	Electrical	-x10 μm^2	- nm	2.3	-	2.7	6.2	1B
This work	Electrical	1x9 μm^2	100 nm	6.5	3.8*	7	45.5	-
This work	Optical 915nm	1x9 μm^2	100 nm	6.11	3.8*	5.9	36	≈ 30k
This work	Optical 915nm	1x5 μm^2	200 nm	6	3.5*	5.25	31.5	≈ 30k

** Calculated on the basis of the conductivity of [10], which equal to 2.9·10^5 S/m.*

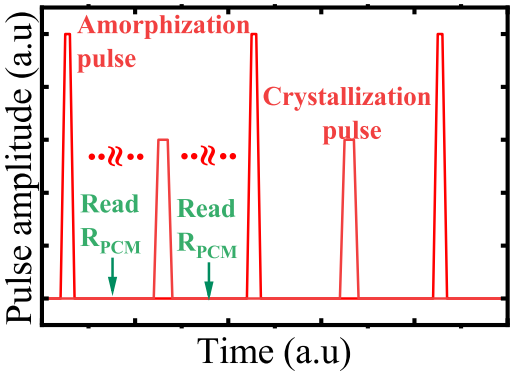

Fig. 5. Schematic timeline of cycling measurement.

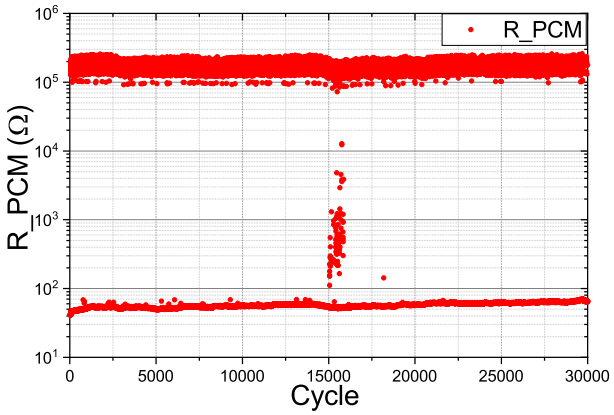

Fig. 6. Switching cycles.

the R_{on} resistance up to 40 GHz, as shown in Fig. 3(b). This representation highlights the decrease in resistance from 12Ω to 6Ω, when the PCM switch cross-section is doubled while keeping the same length of 1 μm. This result confirms theoretical calculations provided in Table 2, underscoring the advantages of wider, thicker PCMs. Fig. 4(a) shows the S-parameters in the OFF state. In this case, the devices are actuated optically with a short pulse to get the amorphous state, which is well described by an isolation greater than 19 dB up to 40 GHz. OFF-state capacitances are extracted in Fig. 4(b). As expected, wider and thicker devices have slightly higher capacitances (between 0.1 and 0.8 fF higher) as the coupling area is doubled. This leads to a Figure of Merit (FoM) of 31.5 fs with a cutoff frequency of 5 THz on DUT15_2 instead of 57.9 fs and 2.75 THz on the DUT15_1 device.

IV. Cycling Test with Optical Actuation

After determining the conditions for optical actuation in the first part, the switch cycle was studied on the DUT25_2 device. Using the setup of Fig. 1(a), with a repetition rate of 4 Hz as in Fig. 5, DC resistance was measured over several hours for the two states after each transition, as shown in Fig. 6. The DC resistor is plotted as a function of the cycle number, and we can see that 30k cycles are achieved with a ratio $R_{off}/R_{on}>10^4$. In addition, both the crystalline and amorphous DC resistance values remain stable throughout the measurements, so the cycle has been successfully completed. Nevertheless, some DC resistance values in the OFF-state can be observed below 10^5 Ω, meaning that GeTe is not in fact in the amorphous state as expected. Specifically, 30 failed amorphization pulses were counted. These PCM amorphization failures are due to micro-vibrations of the positioners that temporally misaligned the fiber, leading to partial PCM amorphization. Even with this limitation in the measurements, this is the first demonstration of an optically actuated PCM switch with so many cycles, where only a dozen cycles have been completed so far [9][11].

V. Discussion

Table 2 compares the switching cycle endurance and the FoM of our work with those published in the literature, considering both electrical and optical excitations. Regarding the optical part, significant performance can be observed in terms of switching cycles. As aforementioned, this is the first time so many cycles have been achieved with optical excitation. A FoM of 31.5 fs is obtained, i.e. only 5.5 fs higher

than in [10], while the DUT15_2 device is three times smaller. This could be explained by a switch in [10] is not totally crystallized, contrary to what we obtained since our results are in line with the theoretical calculations. To confort this assumption, R_{on} in [10] measured is equal to 3 Ω, whereas their geometry and material properties would suggest 1 Ω, if totally crystallized. Furthermore, the optical wavelengths used in the literature present particular challenges in integrated photonics, such as choice of materials, complexity, and fabrication costs, thus limiting their development, which is not the case with 915 nm. In terms of comparison with electrical excitation, we obtained less cycles than [13][15][16]. This is due to external factors such as fiber misalignment after hours of cycling since we did not observe any degradation of our PCM. For the sake of comparison in terms of FoM, we can see that our devices present a FoM comparable the state of art and also better than the one of our device with electrical excitation having the same dimensions and properties of GeTe, improving from 45.5 fs to 36 fs. This can be explained by the excellent control of the crystalline zone during optical excitation, as well as the absence of any heating element which leads to parasitic capacitances, and makes C_{off} bigger.

VI. Conclusion and Perspectives

The optical actuation of a GeTe-based RF switch with different geometries is studied at 915 nm. Switching conditions for ON and OFF states are found. Cycle testing is demonstrated for at least 30k switching cycles, which is the highest optical rate reported so far. Small-signal measurements show lower FoMs for thicker and/or wider switches due to their low ON-state resistance, confirming the advantage of using wider, thicker PCMs by direct optical irradiation. This work paves the way for the realization of high-performance optically actuated RF switches that will further benefit from CMOS-integrated photonics. Typically, integrated photonics at 915 nm relies on a standard back-end process with Si/silica optical waveguides. In this context, the co-integration of PCM RF switches and integrated passive photonics represents a new stage in optical actuation. Ultimately, the realization of a fully integrated optical actuation circuit can be envisaged using hybrid integrated lasers [17].

Acknowledgment

This research was developed with funding from the Presidency of Grenoble Institute of Technology of the University Grenoble Alps and the French Public Authorities within the frame of IPCEI/Nano2022 project.

References

[1] A. Fantini *et al.*, "Comparative Assessment of GST and GeTe Materials for Application to Embedded Phase-Change Memory Devices," in *IEEE International Memory Workshop*, 2009, pp. 1–2. DOI: 10.1109/IMW.2009.5090585.

[2] S. R. Ovshinsky *et al.*, "Reversible Electrical Switching Phenomena in Disordered Structures," in *Phys. Rev. Lett.*, vol. 21, 1968, pp. 1450–1453. DOI: 10.1103/PhysRevLett.21.1450.

[3] A. Naoui *et al.*, "Indirect Electrical-Control Through Heating of a GeTe Phase Change Switch and Its Application to Reflexion Type Phase Shifting," in *International Microwave and Antenna Symposium (IMAS)*, 2023, pp. 13–16. DOI: 10.1109/IMAS55807.2023.10066891.

[4] T. Singh *et al.*, "Miniaturized DC-60 GHz RF PCM GeTe-Based Monolithically Integrated Redundancy Switch Matrix Using T-Type Switching Unit Cells," in *IEEE Transactions on Microwave Theory and Techniques*, vol. 67, 2019, pp. 5181–5190. DOI: 10.1109/TMTT.2019.2944359.

[5] N. El-Hinnawy *et al.*, "12.5 THz Fco GeTe Inline Phase-Change Switch Technology for Reconfigurable RF and Switching Applications," in *2014 IEEE Compound Semiconductor Integrated Circuit Symposium (CSICS)*, 2014, pp. 1–3. DOI: 10.1109/CSICS.2014.6978522.

[6] N Wainstein *et al.*, "Radiofrequency Switches Based on Emerging Resistive Memory Technologies - A Survey," in *Proceedings of the IEEE*, vol. 109, 2020, pp. 77–95.

[7] S. Gharbieh *et al.*, "Phase Change Material Based Reconfigurable Transmitarray: A Feasibility Study," in *16th European Conference on Antennas and Propagation (EuCAP)*, 2022, pp. 1–4. DOI: 10.23919/EuCAP53622.2022.9769642.

[8] I. Charlet *et al.*, "RF Performance of Large Germanium Telluride Switches for Power Application," in *18th European Microwave Integrated Circuits Conference (EuMIC)*, 2023.

[9] L. Chau *et al.*, "Optically Controlled Gete Phase Change Switch And Its Applications in Reconfigurable Antenna Arrays," in *SPIE Defense and Security*, 2016. DOI: 10.1117/12.2179852.

[10] A. Crunteanu *et al.*, "Optical Switching of Gete Phase Change Materials for High-Frequency Applications," in *IEEE MTT-S International Microwave Workshop Series on Advanced Materials and Processes for RF and THz Applications (IMWS-AMP)*, 2017, pp. 1–3. DOI: 10.1109/IMWS-AMP.2017.8247379.

[11] M. Pinaud *et al.*, "Terahertz Devices Using the Optical Activation of GeTe Phase Change Materials: Toward Fully Reconfigurable Functionalities," in *ACS Photonics*, vol. 8, 2021, pp. 3272–3281. DOI: 10.1021/acsphotonics.1c01086.

[12] N. El-Hinnawy *et al.*, "A Four-Terminal, Inline, Chalcogenide Phase-Change RF Switch Using an Independent Resistive Heater for Thermal Actuation," in *IEEE Electron Device Letters*, vol. 34, 2013, pp. 1313–1315. DOI: 10.1109/LED.2013.2278816.

[13] J.-S. Moon *et al.*, "Phase-change RF switches with robust switching cycle endurance," in *IEEE Radio and Wireless Symposium (RWS)*, 2018, pp. 231–233. DOI: 10.1109/RWS.2018.8304995.

[14] M. Wang *et al.*, "Directly heated four-terminal phase change switches," in *IEEE MTT-S International Microwave Symposium*, 2014, pp. 1–4. DOI: 10.1109/MWSYM.2014.6848367.

[15] J.-S. Moon *et al.*, "5 THz Figure-of-Merit Reliable Phase-change RF Switches for Millimeter-wave Applications," in *2018 IEEE/MTT-S International Microwave Symposium - IMS*, 2018, pp. 836–838. DOI: 10.1109/MWSYM.2018.8439479.

[16] N. El-Hinnawy *et al.*, "A 25 THz F_{CO} (6.3 fs $R_{ON} * C_{OFF}$) Phase-Change Material RF Switch Fabricated in a High Volume Manufacturing Environment with Demonstrated Cycling > 1 Billion Times," in *IEEE/MTT-S International Microwave Symposium (IMS)*, 2020, pp. 45–48. DOI: 10.1109/IMS30576.2020.9223973.

[17] A. Marinins *et al.*, "Wafer-Scale Hybrid Integration of InP DFB Lasers on Si Photonics by Flip-Chip Bonding With sub-300 nm Alignment Precision," in *IEEE Journal of Selected Topics in Quantum Electronics*, vol. 29, 2023, pp. 1–11. DOI: 10.1109/JSTQE.2022.3223641.